Electric Power Systems Research 214 (2023) 108808

Contents lists available at ScienceDirect

Electric Power Systems Research

journal homepage: www.elsevier.com/locate/epsr

An innovative mode-based coherency evaluation method for data-driven controlled islanding in power systems

Mohamadsadegh Sadeghi [a], Hamidreza Akbari [a,*], Tahereh Daemi [a], Somayeh Mousavi [b]

[a] Department of Electrical Engineering, Yazd Branch, Islamic Azad University, Yazd, Iran
[b] Department of Industrial Engineering, Meybod University, Meybod, Iran

ARTICLE INFO

Keywords:
Coherency evaluation
Complex domain
Controlled islanding

ABSTRACT

Controlled islanding is considered the last remedial action for preventing power systems from moving toward collapsing. In this respect, power systems should be split into islands, so that each island remains stable from both static and dynamic viewpoints. Therefore, determining the center of each island and its load bus borders is a fundamental task. In this paper, an innovative method is presented to determine the appropriate islanding scheme following the occurrence of a disturbance. This method is based on excited modes and it uses density-based learning approaches to cluster buses of the system in complex planes. The clustering process is performed with respect to each central bus to find candidate area borders. This is crucial, since wide area post disturbance control actions and restoration can be more effective in this way. Additionally, the proposed coherency evaluation method is incorporated into the static load flow analysis to form an optimization problem for determining the borders of each island. Accordingly, both static and dynamic aspects of islands are included in the problem from a control-based viewpoint. The results of applying the proposed approach on test cases demonstrate its effectiveness.

1. Introduction

Nowadays, modern power systems (or smart grids) are encountering challenges that affect their secure and stable operation [1]. Such challenges may cause the power system to move toward an unstable operation condition following a disturbance occurrence and then results in a series of cascading outages that can eventually lead to a major blackout in the system. In order to prevent any blackout in the system, controlled islanding is considered as the last corrective action [2,3]. However, applying an appropriate islanding scheme, which considers both dynamics and statics of the system, has always been a challenge. This issue becomes more challenging when distributed generations (DGs) with uncertainties in their outputs exist, especially in distribution systems [4].

Generally, the basics of controlled islanding in transmission systems are different from those of distribution systems. In transmission systems, controlled islanding is applied to the system, so that each island can operate securely from both dynamic and static viewpoints. Controlled islanding in transmission systems is dealt with identifying coherency degrees in the system [5,6]. Coherency is the similarity of responses in the system following a disturbance, which is represented primarily by oscillations in the rotor angle or speed signals of generators [7,8]. Although modal-based methods like the slow-coherency method were first introduced for coherency evaluation [9], today the advent of online monitoring systems such as wide area measurement system has made it possible to use data driven coherency analysis methods (which are also called measurement-based methods) for online coherency evaluation [10,11]. In measurement-based methods, following a disturbance occurrence, the required data are measured across the power system and then are processed for coherency evaluation. In doing so, operations such as principal component analysis [12], cosine similarity evaluation [13], projection pursuit [14], etc. have been proposed for processing the measured data. A comprehensive review of coherency evaluation methods has been provided in [15].

In the literature, various methods have been presented for the controlled islanding of power systems. Broadly speaking, these methods can be divided into two main categories. The methods in the first category use the Graph theory to split a large power system into islands [16–20]. Ref. [18] provides the details of using graph theory in power system islanding. In another study presented in [19] weighted time varying graphs are utilized in order to determine the boundaries of islands. Another concept called graph spectra has been employed in [20]

* Corresponding author.
E-mail address: h.akbari@iauyazd.ac.ir (H. Akbari).

https://doi.org/10.1016/j.epsr.2022.108808
Received 24 July 2022; Received in revised form 29 August 2022; Accepted 10 September 2022
Available online 18 September 2022
0378-7796/

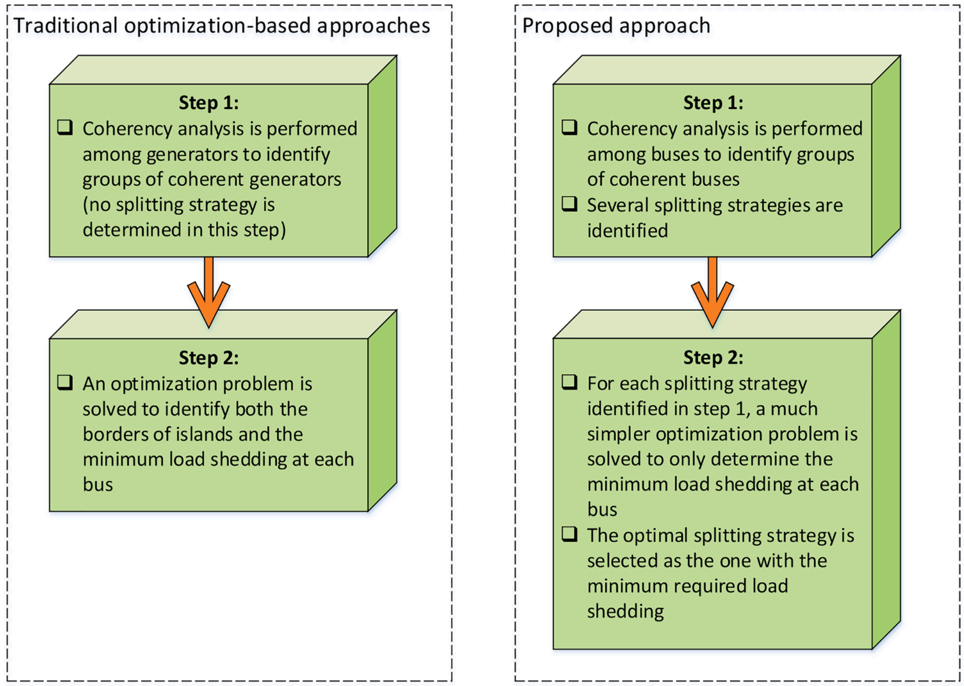

Fig. 1. Comparison between the steps of the proposed approach and traditional approaches.

to find the islanding strategy in a system highly penetrated with renewable generation. Authors in [21] have presented an optimization methodology for specifying the intentional islanding strategy in which graph theory-based network reduction technique is used to improve the computational efficacy of the model. In the second category, methods are placed that employ mixed integer programming to solve an optimization problem which its solution is an optimal islanding strategy [22–32]. The purpose of these optimization problems is to minimize power imbalance or dynamic coupling or power flow disruption [30]. For example, in [22] DC load flow as the simplest formulation of power flow balance has been employed in mixed integer linear programming (MILP) formulation to find the optimal islanding strategy. However, since a linear AC formulation can better represent the system constraints (mostly in terms of power losses which should not be ignored), Ref. [23] has considered the linear AC power flow in their linear optimization formulation. Authors in [25] have used an MILP optimization model based on the linearized ac power flow to find the optimal island boundaries and guarantee the efficient isolation of critical or most affected islands by detection of generators most affected by the disturbance. The impacts of uncertainties brought by renewable generation on the generation-demand balance required for establishing a correct islanding condition have been addressed in [26]. A method for optimal power system splitting based on mixed integer programming has been developed in [29] which also considers the system restoration constraints. In another work presented in [6], authors have presented a methodology for intentional controlled islanding using a MILP model in which transient stability constraints are combined with voltage stability constraints. Other technical aspects such as the impact of false data injections attack on correct controlled islanding of power systems have been investigated in [31]. Recently, the use of convolutional neural networks in intentional power system islanding has been investigated in [32].

It is worthy to note that, nevertheless the above-mentioned works uses either graph theory or optimization approaches (or a combination of them such as the one presented in [21]), the use of both slow-coherency and online coherency concepts have been reported in both categories [33–35]. Recently, the use of data driven methods for online coherency evaluation incorporated into mixed linear programming models for finding the controlled islanding strategy has been proposed [27,36]. First, this method is suggested in the related literature to find coherent generators, and then the obtained coherency between generators is added to the optimization problem as a dis-connectivity constraint.

However, it should be noted that in all previous studies in the second category, islands' borders have been determined in the solution of an optimization problem, aiming at minimizing the amount of load shedding at buses [37]. In other words, maintaining the static stability of an island has played the main role in finding the best controlled islanding solution in the papers published thus far. After a disturbance occurs in the system, generators will respond to the disturbance, which is represented by the variations in their rotor angle or speed signals. The response of a generator is also propagated in the system and is reflected by variations in voltage and current phasors at buses and lines. Consequently, voltage phasors measured at buses closer to a generator exhibit more similar variations in their amplitude or phase angles. In other words, analysis of the variations in voltage phasors can help to find how far the response of coherent groups of generators has been propagated in the system [38,39]. In the proposed approach, coherency evaluation is carried out on the phase angle variation of buses rather than on the rotor angle or speed of generators. By doing so, we are capable to find the boundaries in the first step and therefore simplify the optimization problem in the second step by removing the auxiliary variables associated to dis-connectivity of buses.

In the other hand, a new look at the coherency evaluation among buses in the complex plane is introduced in this paper. This new way of coherency evaluation enables us to evaluate coherency from the view point of each central bus. By doing so, buses will be located at different places in the complex planes, meaning that the degree of coherency between two buses (the distance between their location in the complex plane) is dependent to their similarity with the cluster centers. In other words, in the proposed approach, coherency between each two buses is evaluated from a system-wide point of view rather than solely relying on the data of the two buses. Accordingly, using this new concept it will be able to obtain a candidate splitting strategy from the view point of each central bus. Then, the simplified optimization problem will calculate the load shedding for each of the given candidate splitting strategies to determine which one leads to the least amount of the load shedding, i.e. the best strategy as the final solution.

In summary, the contributions of this paper are as follows.

- Instead of finding coherency between generators, this paper evaluates the coherency between buses of the system. Hence, some candidate splitting schemes will be obtained, which are then analyzed for finding the best of them. Note that, in the proposed approach, the aim is to move the focus of the controlled islanding problem to the dynamics of the system. Such approach have simplified the mixed linear optimization problem, such that more than half of variables used in previous works have been omitted.
- In the proposed approach, coherency is assessed from the view point of each central bus. In other words, coherency between each two buses is evaluated from a system-wide point of view rather than solely using the data measured at the two buses.
- The proposed approach uses data measured to analyze coherency based on the similarity of excited modes. Therefore, a novel coherency evaluation in the complex domain is proposed, which uses a density-based unsupervised learning technique called density-based spatial clustering of applications with noise (DBSCAN), which is described in [40] to find clusters in each complex domain. DBSCAN has advantages over other conventional clustering methods, such as fuzzy c-means (FCM) and k-means (KM) algorithms, causing it to be an appropriate technique for this online coherency evaluation application. Section 2.1 will present the features of DBSCAN.
- By using the proposed coherency evaluation approach, several candidate splitting schemes will be determined in advance, and then the best of them is detected as the one leading to less amount of load shedding. Thus, as the borders of islands are determined based on the propagation of responses of generators in the system, tuning the controllers during islanding and when restoration is carried out will be more effective.

The rest of paper is organized as follows: In Section 2, the proposed methodology for online power system controlled islanding is presented. Section 3 is dedicated to demonstrate the validation of the proposed methodology using two different cases. A discussion is also provided in Section 3. Finally, conclusions are presented in Section 4.

2. Proposed methodology for online power system controlled islanding

The approach proposed in this paper for controlled islanding is an optimization-based approach like those presented in [28] and [35] which are here called traditional approaches. As Fig. 1 depicts, both the proposed approach and traditional approaches consist of two steps. This figure shows the features of each step of the approaches. In traditional approaches, following the occurrence of a disturbance, the coherency is evaluated among generators, and then groups of coherent generators are identified. Note that no splitting strategy is determined in this step. Then, in the second step, a general optimization problem is solved to find the optimal splitting strategy considering the groups of coherent generators identified in the previous step. Note that the optimization problem defined in traditional approaches is solved for numerous variables, including those related to the dis-connectivity of buses.

However, in the first step of the proposed approach, candidate-splitting strategies are identified using a density-based unsupervised learning technique applied to data points in separate complex planes. Then, in the second step, an optimization problem is solved for each strategy to find the best one in terms of the minimum load shedding required to maintain each island securely in operation. The two steps of the proposed approach will be discussed in the following subsections:

2.1. Coherency evaluation in the complex domain

In this paper, coherency is evaluated from a data-driven viewpoint, since previously slow-coherency-based approaches have been proven not to be applicable in practical applications. The coherency evaluation approach presented in this section is based on excited modes and therefore it is suitable for control actions before and during controlled islanding. It is assumed that all required data, including voltage phasor signals are securely available through the wide area measurement system. Thus, discrete Fourier transform (DFT) can be applied to these signals as in (1) to extract the frequency components existing in them [41].

$$F_i(f) = \sum_{k=0}^{N-1} \delta_i(k) e^{-\left(j\frac{2\pi fk}{N}\right)} f = 0, 1, ..., N-1 \tag{1}$$

where δ_i is the phase angle of the voltage phasor at the ith bus, and N is the number of samples in the time window. A traditional and effective way to assess the similarity of x_i and x_j, which are two vectors each of them with N real values, is to use the Pearson correlation coefficient (CC) defined in (2) [42].

$$cc_{i,j} = \frac{\sum_{k=1}^{N} x_i(k) x_j(k)}{\sqrt{\sum_{k=1}^{N} x_i^2(k) \sum_{k=1}^{N} x_j^2(k)}} \tag{2}$$

Using (2) for the two vectors x_i and x_j which have real components, the value of $cc_{i,j}$ will be real as well and with a value between 1 (for two in phase real vectors) and -1 (for two out of phase real vectors). However, since the frequency spectrum obtained from applying DFT, i.e. $F(f)$, is a vector with complex components, the value of $cc_{i,j}$between two complex vectors, which in this paper correspond to buses i and j, will be a complex value as well using (2). Interpretation of the values of $cc_{i,j}$ obtained from (2) is not easy as it may leads to complex values greater than 1. To solve this problem and more importantly to consider the effects of phase difference in each frequency component, the following form of $cc_{i,j}$ defined in (3) will be utilized in which the inner production of complex vectors (the (.) production) is used in the numerator in order to include the phase difference of each element of complex vectors; this is essential for mode-based coherency evaluation [43].

$$cc_{i,j} = \frac{F_i(f).F_j(f)}{\sqrt{\sum_{f=1}^{N} |F_i(f)|^2 \sum_{f=1}^{N} |F_j(f)|^2}} \tag{3}$$

Thus, the value of $cc_{i,j}$ obtained using (3) will be a complex value with a magnitude between [0, 1] and an angle between [0°, 360°]. Accordingly, it would be easier to evaluate the coherency between two buses or generators. Obviously, the more the CC's value is close to 1 + j0, the more the two complex vectors are similar, and therefore the more the two buses are probable to be in the same area based on excited modes.

To find coherent buses, the proposed approach uses a combination of two density-based methods, one using the real values to find the number of clusters and their centers and another one to find the borders of each area. Note that both methods act in the complex domain. Given the angular velocity of voltage phasors of all buses, in the first step, the similarity between each pair of them is calculated using the Pearson correlation coefficient. Then, a density value is calculated for each bus using the following density measure [44].

$$D_i = \sum_{j=1}^{N_B} e^{-\left(\frac{d_{i,j}}{r_a/2}\right)^2} i = 1, ..., N_B \tag{4}$$

where N_B is the number of buses in the system and r_a is a positive constant used to represent the desired neighboring radius. In addition, $d_{i,j}$ is the dissimilarity index defined as $d_{i,j} = |1 - cc_{i,j}|$. According to (4), the

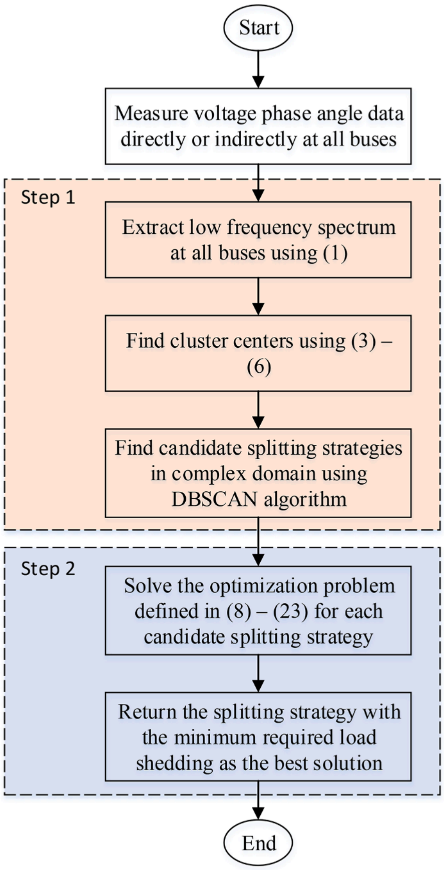

Fig. 2. Flowchart of the proposed approach.

value of D for a bus that owns a high similarity in its variation with a large number of buses will be high. Hence, the bus having the highest density value is regarded as the first cluster center. Having obtained the first cluster center, the following subtractive operation is conducted to revise the density values with respect to the similarity of buses with the first cluster center. Thus, the second cluster center will be determined as the one that has the highest value among the revised density values [44].

$$D_i^h = D_i^{h-1} - D_C^{h-1} \times e^{-\left(\frac{d_{i,C_{h-1}}}{r_b/2}\right)^2} \quad i = 1, 2, \ldots, N_B \tag{5}$$

In (5), D_C^{h-1} is the density value of the cluster center identified in the iteration $h-1$, $d_{i,C_{h-1}}$ is the value of the dissimilarity index calculated between bus i and the central bus (cluster center) identified in the iteration $h-1$. Moreover, r_b is a positive constant used to define the neighborhood that has measurable reductions in density values. Note that the ratio of r_b to r_a must be greater than 1. The above process is then repeated until the rejection factor rejects the new center. A rejection factor can be simply defined as in (6) [44].

$$\frac{D_C^h}{D_C^1} \geq \lambda \tag{6}$$

Having obtained N_C clusters centers, the next step is triggered in the complex domain to achieve N_C candidate strategies. Then, N_C set of complex values are created as follows:

$$\Omega_i = \{ cc_{1,i} \quad cc_{2,i} \quad \ldots \quad cc_{N_B,i} \} i = 1, \ldots, N_C \tag{7}$$

where $cc_{j,i}$ is the correlation coefficient between the j^{th} bus and i^{th} cluster center (central bus). Then, the elements of Ω_i, which are complex values, are depicted in the complex plane. In other words, we will have N_C illustrations of complex values in the complex plane, so that each one corresponds to one cluster center. For example, if only two central buses are obtained for a system with N_B buses, then there would be two 2D complex plane illustrations. In the first one, N_B data points are depicted, which correspond to the correlation coefficient values obtained between

Table 1
Parameters used in the simulations and their values.

Parameter	Value
r_a	0.5
r_b	$1.5 \times r_a$
λ	0.2
minPt	2
α	0.15
$V_i^{\max}$	1.05 pu
$V_i^{\min}$	0.95 pu

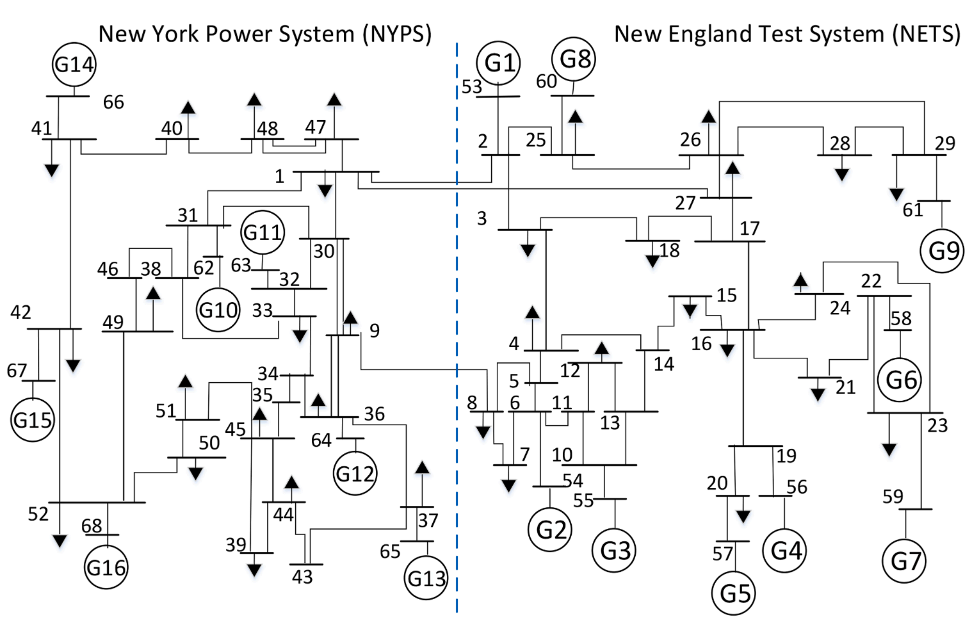

Fig. 3. Single line diagram of the test system.

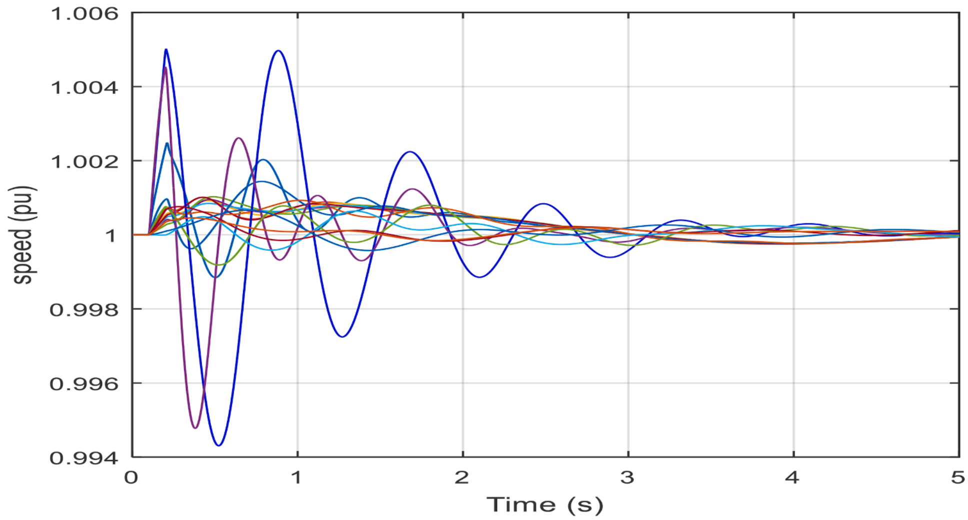

Fig. 4. Rotor speed variations in Case 1.

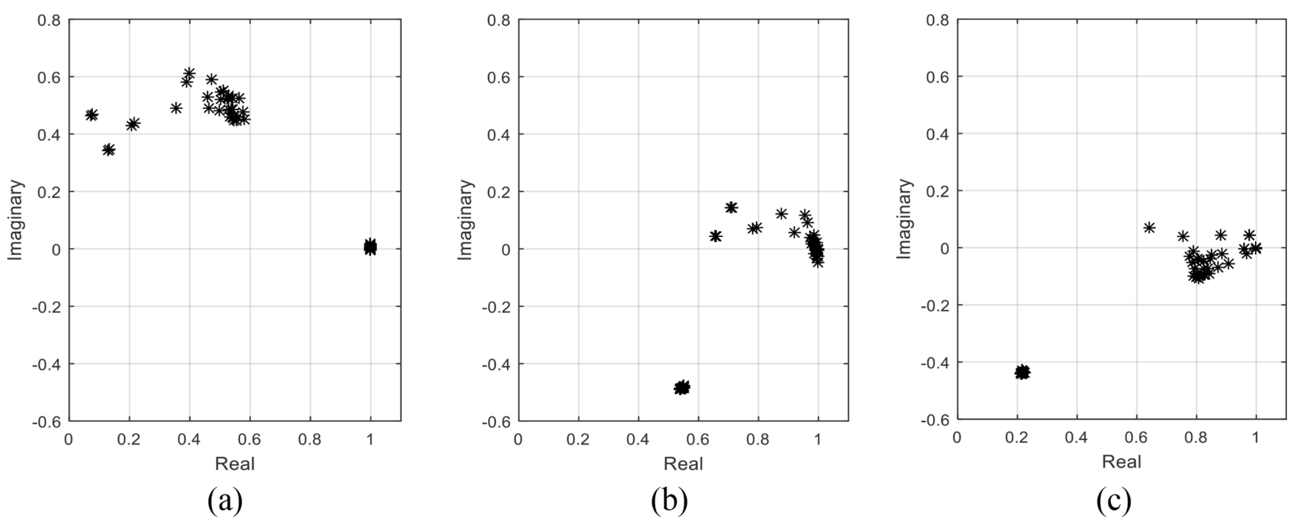

Fig. 5. Locations of complex CCs in the complex domain (a) with respect to bus 21 (b) with respect to bus 64 and (c) with respect to bus 52.

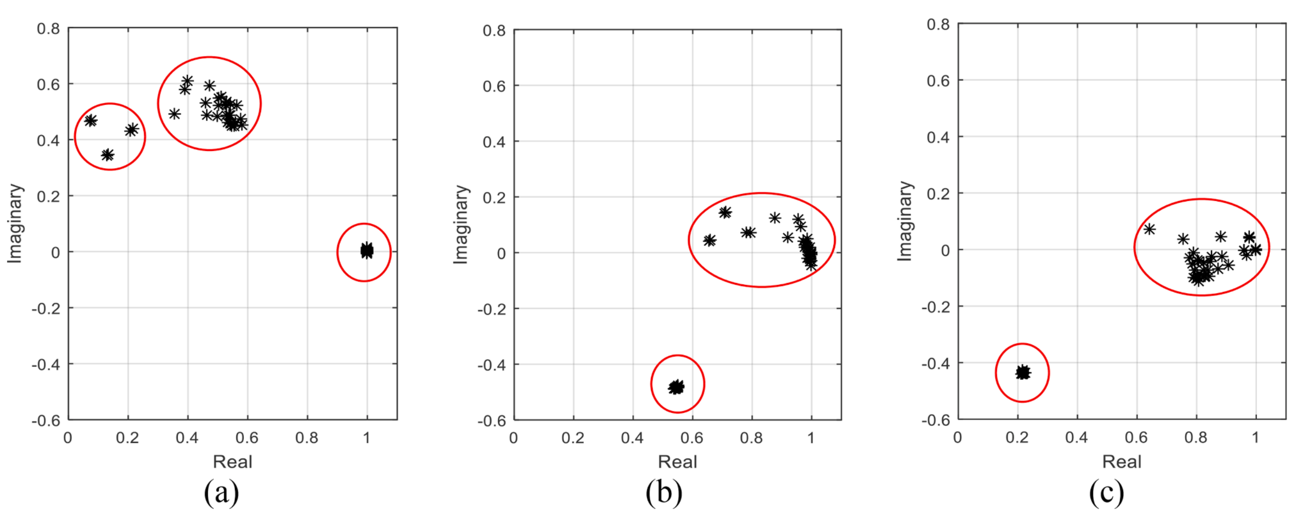

Fig. 6. Clusters identified by DBSCAN in Case 1, (a) with respect to bus 21 (b) with respect to bus 64 and (c) with respect to bus 52.

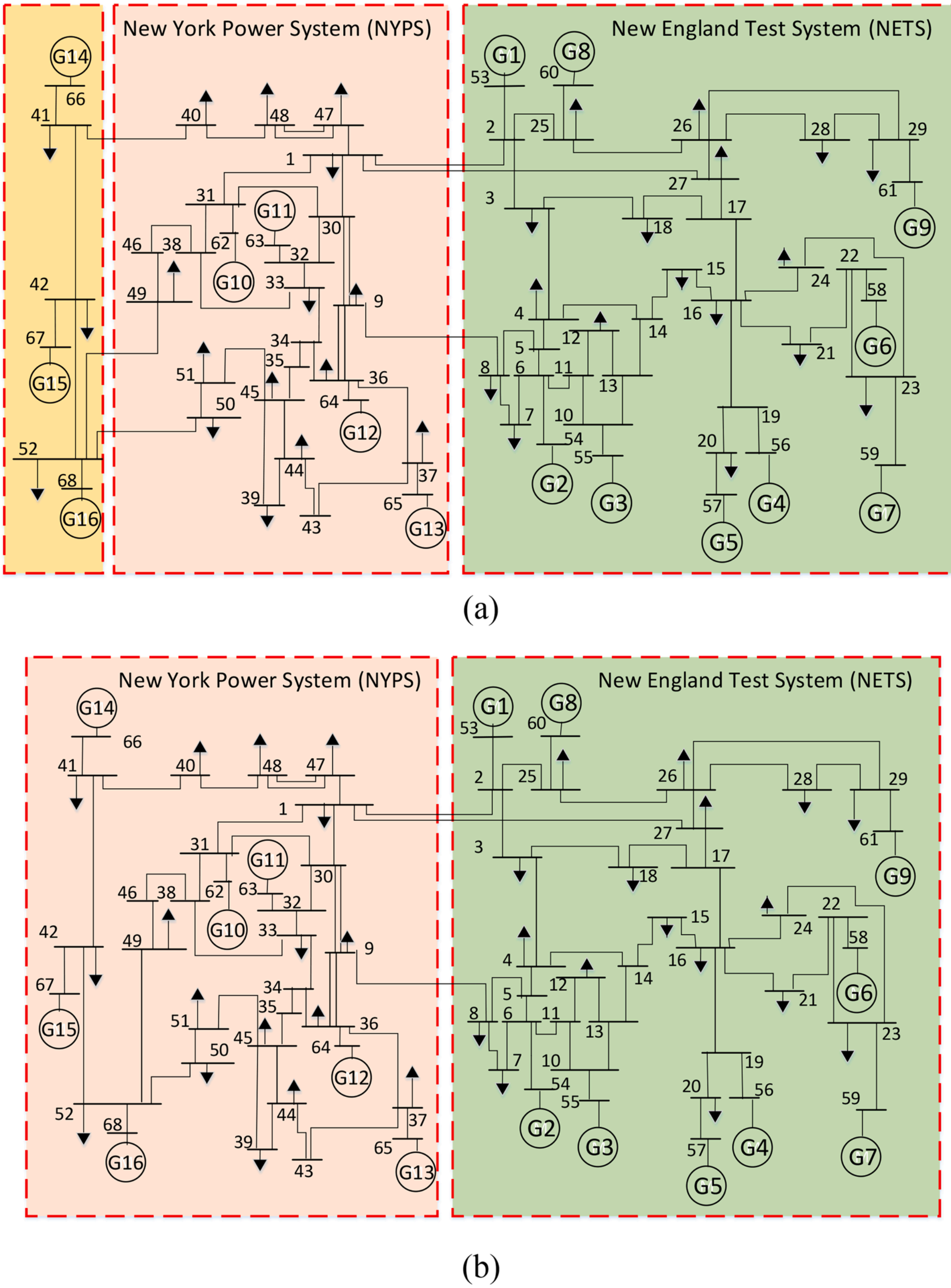

Fig. 7. Areas identified in Case 1, (a) with respect to bus 21 (b) with respect to either bus 64 or bus 52.

Table 2
Load shedding results (case 1).

	Scheme 1			Scheme 2	
	Area 1	Area 2	Area 3	Area 1	Area 2
Load shedding in each area (MW)	0	11	0	0	0
Total (MW)	11			0	

the first central bus and the rest of buses, while in the second illustrations, the N_B data points are the correlation coefficient values between the second central bus and the rest of buses.

Once the correlation coefficient values as data points are depicted in the complex domain, DBSCAN is applied to cluster them. For a transmission system with tens or hundreds of buses, it is impossible to cluster the buses visually. Therefore, it is needed to employ an appropriate clustering algorithm. Among various types of clustering algorithms, such as k-means clustering (KM), fuzzy c-means (FCM), and fuzzy c-medoid (FCMd) clustering, DBSCAN is the one suitable for the proposed approach. Indeed, DBSCAN has advantages over other clustering

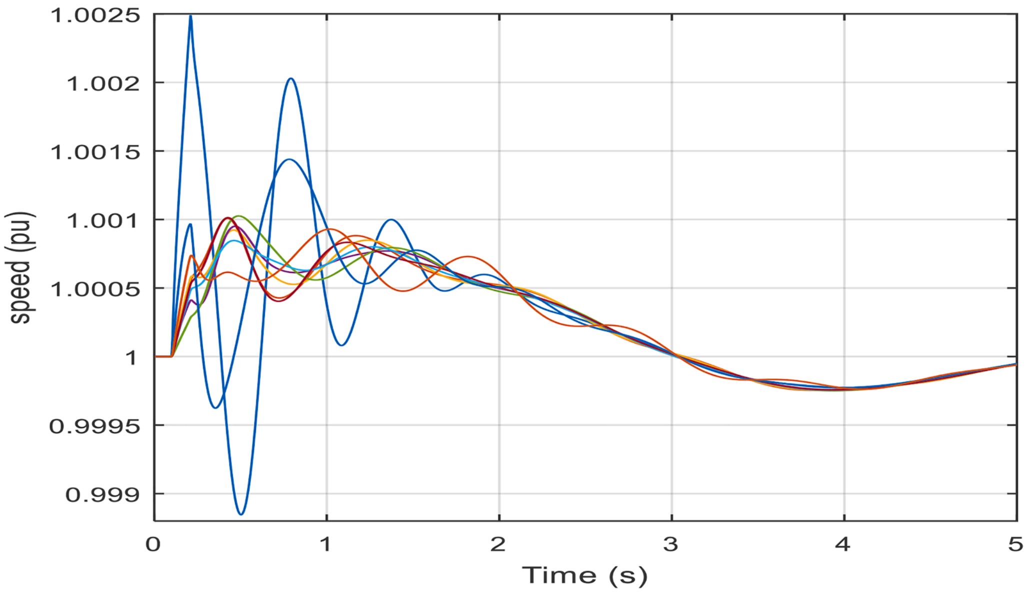

Fig. 8. Rotor speed variations of generators G1 – G9.

algorithms, such as FCM and KM, as follows: (i) unlike KM and FCM, DBSCAN does not need any prior assumption on the number of clusters in the dataset, (ii) DBSCAN can easily find small clusters in the dataset; this is not always practical, when using KM and FCM, (iii) the solution obtained by DBSCAN is deterministic.

Note that when using DBSCAN, two parameters, i.e. a radius for determining the neighborhood (α) and the minimum number of data points required to exist in the α-neighborhood of a data point to form a cluster (minPt), are needed to be tuned. Also, note that in the case of coherency assessment application, there is a difference between applying DBSCAN to correlation coefficient values obtained from real vectors and complex vectors. In other words, in the complex domain, there is the possibility to discriminate between other coherent groups swinging against the under study coherent group, which is impossible when using real vectors. This means that applying DBSCAN to the complex correlation coefficient values provides a better view of coherency and non-coherency among the buses. This can also be seen in the test cases simulated in Section 3.

2.2. Mixed integer linear approach for load shedding in candidate islands

As described in Section 1, in conventional optimization-based methods coherency is evaluated between rotor angle or speed of generators. Accordingly, before solving the optimization problem, only sets of coherent generators are determined. However, the borders of each island within which coherent generators do exist are not determined yet. Therefore, in conventional methods an optimization problem has been solved not only to find the borders of islands but to calculate the least amount of load shedding required in each island. In order to do that, a set of auxiliary variables have been added to the problem to make sure that coherent generators remain in an island. Additionally, another set of auxiliary variables have been also used to reflect the connection of buses. These additional auxiliary variables are binary, meaning that the unity values means connectivity and vice versa. Hence, as it can be seen, too many auxiliary variables have been included in the optimization problem used by conventional methods. However, in the proposed method these auxiliary variables do not exist since the borders of islands are known (a few candidate islanding strategies are determined beforehand) and thus the optimization problem only calculates the optimum load shedding required in each island.

After determining the candidate islanding strategies in step 1, it is now necessary to calculate the minimum amount of load shedding required at each load bus in each island so that load flow constraints of the island are satisfied. This is a necessary task to make sure that in each island the load-generation remains in balance. In doing so, the objective function of the proposed optimization problem, which is aimed to minimize the required amount of load shedding, will be as follows:

$$\min \sum_{s=1}^{N_S} \sum_{i \in \Omega_S} \Delta P^i \tag{8}$$

where ΔP^i is the amount of load curtailed at the ith bus. Constraints used in this problem consist of those related to the remaining power balance in each island. Note that, unlike many previous works in which additional variables were added to the problem to represent the connectivity of buses and the disconnectivity of non-coherent generators, our problem defined in this paper is free from these auxiliary variables. Additionally, although the use of AC load flow constraints, which are nonlinear, leads to a high level of accuracy, the use of a linear approximation will expedite the procedure of solving the problem, while a satisfactory level of accuracy is obtained. The linearized model of AC active and reactive power flow equations defined in (9) and (10) can be obtained from the Taylor expansion as in (11) and (12) [28].

$$P_{ij} = V_i V_j \left(G_{ij} \cos\delta_{ij} + B_{ij} \sin\delta_{ij} \right) - V_i^2 G_{ij} \tag{9}$$

$$Q_{ij} = V_i V_j \left(G_{ij} \sin\delta_{ij} - B_{ij} \cos\delta_{ij} \right) + V_i^2 \left(B_{ij} - \frac{B_{ij}^{sh}}{2} \right) \tag{10}$$

$$P_{ij} = G_{ij} \left(V_i + V_j - 1 \right) + B_{ij} \delta_{ij} + G_{ij} (1 - 2V_i) \tag{11}$$

$$Q_{ij} = G_{ij} \delta_{ij} - B_{ij} \left(V_i + V_j - 1 \right) + (2V_i - 1) \left(B_{ij} - \frac{B_{ij}^{sh}}{2} \right) \tag{12}$$

Having linearized the power flow equations, the active and reactive power balance equations at the ith bus will be defined as follows:

$$P_i = \sum P_{ij} = P_{G,i} + \Delta P_{G,i}^{up} - \Delta P_{G,i}^{down} - P_{L,i} + \Delta P_{L,i}^{sh} \tag{13}$$

$$Q_i = \sum Q_{ij} = Q_{G,i} + \Delta Q_{G,i}^{up} - \Delta Q_{G,i}^{down} - Q_{L,i} + \Delta Q_{L,i}^{sh} \tag{14}$$

where $\Delta Q_{L,i}^{sh}$ is the amount of reactive load curtailment, $\Delta P_{G,i}^{up}$ and $\Delta P_{G,i}^{down}$ are the amounts of increase and decrease in active power generations,

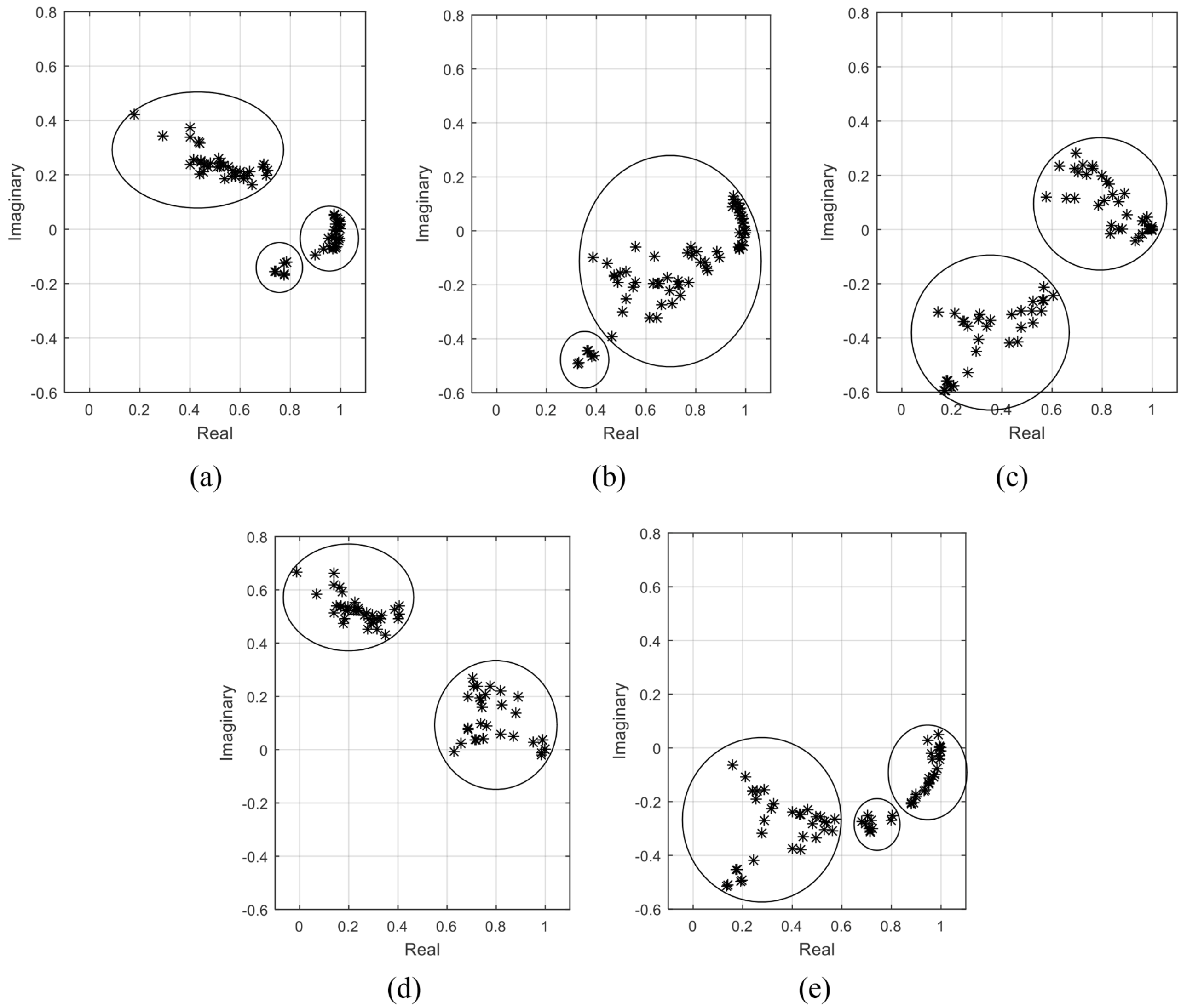

Fig. 9. Clusters identified by DBSCAN in Case 2, (a) with respect to bus 33 (b) with respect to bus 26 (c) with respect to bus 11 (d) with respect to bus 42 and (e) with respect to bus 23.

and $\Delta Q^{up}_{G,i}$ and $\Delta Q^{down}_{G,i}$ are the amounts of increase and decrease in reactive power generations all at the ith bus. In addition to the constraints defined in (9) - (14), operational limits should also be defined. In this regard, limits on the output of generators as well as amount of short time increase and decrease in generators' output active and reactive powers can be defined as follows:

$$P^{\min}_{G,i} \le P_{G,i} + \Delta P^{up}_{G,i} - \Delta P^{down}_{G,i} \le P^{\max}_{G,i} \tag{15}$$

$$Q^{\min}_{G,i} \le Q_{G,i} + \Delta Q^{up}_{G,i} - \Delta Q^{down}_{G,i} \le Q^{\max}_{G,i} \tag{16}$$

$$0 \le \Delta P^{up}_{G,i} \le \Delta P^{up,\max}_{G,i} \tag{17}$$

$$0 \le \Delta P^{down}_{G,i} \le \Delta P^{down,\max}_{G,i} \tag{18}$$

$$0 \le \Delta Q^{up}_{G,i} \le \Delta Q^{up,\max}_{G,i} \tag{19}$$

$$0 \le \Delta Q^{down}_{G,i} \le \Delta Q^{down,\max}_{G,i} \tag{20}$$

It is obvious that the amount of load shedding is limited to the original load. Accordingly, the following limits can be considered.

$$0 \le \Delta P^{sh}_{L,i} \le P_{L,i} \tag{21}$$

$$0 \le \Delta Q^{sh}_{L,i} \le Q_{L,i} \tag{22}$$

Note that since loads are modeled as constant PQ loads, the constraint on the reactive load shedding can be removed if the same percentage of active load shedding is considered for the reactive load, or in other words, $\Delta Q^{sh}_{L,i} = \Delta Q^{sh}_{L,i} \times \tan\varphi_i$. Another limit used to maintain the voltage stability of the system is defined in (22) to assure that the voltage values remain within the secure range.

$$V^{\min}_i \le V_i \le V^{\max}_i \tag{23}$$

Accordingly, for a given splitting strategy in which the system is split into islands from a dynamic viewpoint, the optimization problem defined in (8) – (23) is solved for each island to find the minimum amount of load shedding required in the island in order to ensure that, in addition to dynamic stability, each island remains stable statically after load shedding is applied.

After solving the optimization problem defined in (8) – (23) for all candidate splitting strategies obtained in the previous step (defined in Section 2.1), the best strategy is then determined as the one leading to the least required amount of load shedding. Fig. 2 depicts the flowchart of the proposed controlled islanding approach. Simulations conducted in the next section will better describe the steps of the proposed approach.

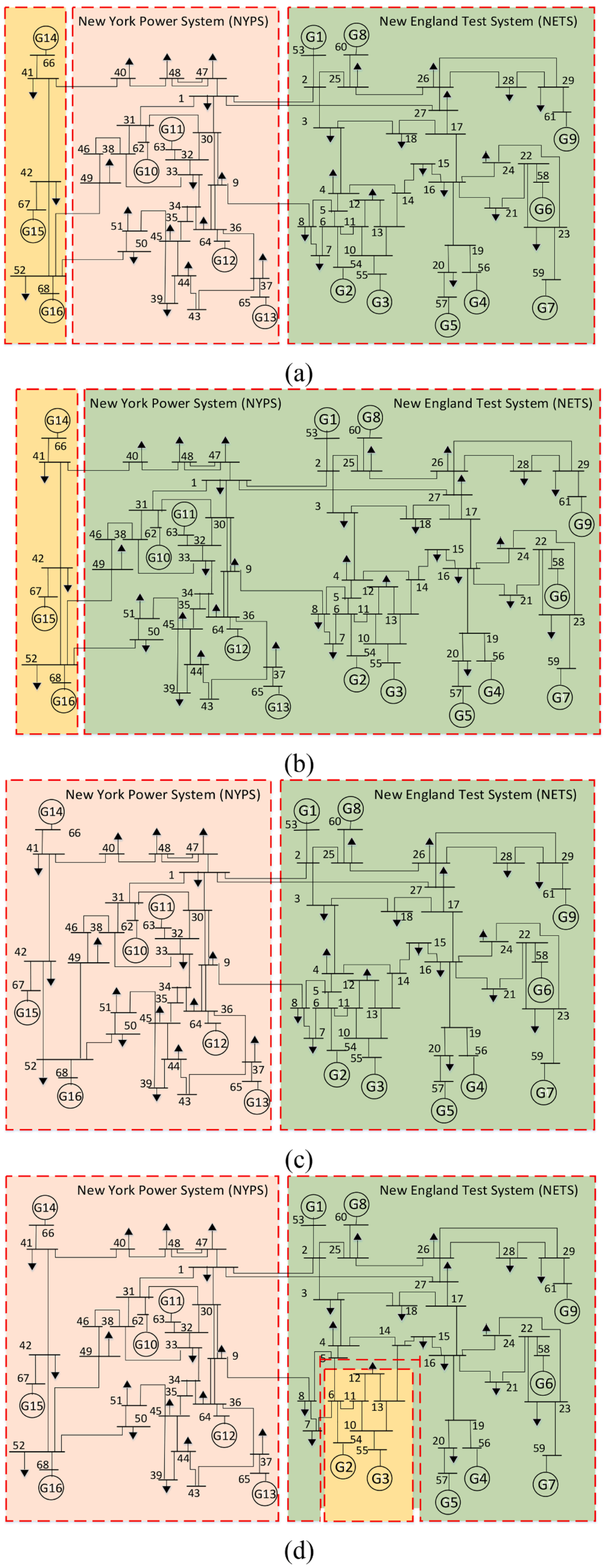

Fig. 10. Areas identified in Case 2, (a) with respect to bus 33 (b) with respect to bus 26 (c) with respect to either bus 11 or bus 42 and (d) with respect to bus 23.

3. Simulation results

In this paper, the controlled islanding approach proposed in Section 2 is applied to the 68-bus, 16-machine system shown in Fig. 3. This system consists of two areas called New England Test system (NETS) and New York Power System (NYPS). Note that generators 14 – 16 are virtual large generators used to represent the dynamic characteristics of areas adjacent to NYPS. More details about this system can be found in [45]. It should also be noted that all simulations were performed in the MATLAB software. Dynamic and time domain simulations were conducted using the Power System Toolbox (PST) available in [46].

Table 1 provides the values of parameters used in this simulations. It should be noted that in order to obtain cluster centers, r_a, r_b and λ are set on 0.5, $1.5 \times r_a$ and 0.2, respectively, according to [44,47]. These values are selected to avoid the formation of closely spaced areas and to ensure that small areas without any generation will not be formed. Parameter associated with the limitations on the active and reactive power increase and decrease in generators, i.e. $\Delta P_{G,i}^{up,\max}$, $\Delta P_{G,i}^{down,\max}$, $\Delta Q_{G,i}^{up,\max}$ and $\Delta Q_{G,i}^{down,\max}$, are assumed to be 20% of the generators' nominal power available in [45]. Furthermore, minPt and α are set on 2 and 0.15, respectively. This means that at least two buses with Euclidean distance less than 0.15 can form an area.

It should also be noted that, time duration of voltage phasor sampling used for coherency evaluation is assumed to be 10 s after fault occurrence. This time duration will allow us to extract low frequencies higher than 0.1 Hz to 2 Hz, which are associated with inter-area and local oscillation modes. Note that smaller time windows can also be considered; however, some low frequencies may not be accurately observable for smaller windows. For example, if a time window of 5 s is selected to be used for coherency evaluation, frequencies lower than 0.2 Hz are not observable anymore.

Two test cases were simulated in this paper. The two cases include two different faults occurring in two different parts of the system to show how the proposed approach can effectively find the solution. In this regard, the aim is to show that coherency evaluation is necessary to be conducted online using data-driven methods in modern power systems.

3.1. Case 1

It is assumed in this case that after disconnecting the line between buses 8 and 9, which is done to increase the electrical distance between the NETS and NYPS, a 3-phase fault is occurred on the line connecting buses 1 and 2 and near to bus 2 and then is cleared after 0.3 s. It is also assumed that no line is tripped out. Fig. 4 shows the post disturbance speed variation of the generators.

By applying the procedure described in Section 2.1, buses 21, 64 and 52 are found to be the cluster centers, meaning that there could be three clusters (or probable islands if necessary) following the occurrence of this fault. In this regard, it is then necessary to analyze the similarity between buses in three separate complex planes. Fig. 5 show the locations of complex CCs between the phase angle variations measured at buses of the system and phase angle variations measured at buses 21, 64 and 52 (cluster centers).

In the first step, DBSCAN is applied to the data points at each complex plane. Clusters obtained after applying DBSCAN are shown in Fig. 6. It can be seen that two clusters have been found in Figs. 6(b) and 6 (c), whereas three clusters have been identified in Fig. 6(a). Therefore, two splitting schemes have been identified in this case and will be then analyzed in the next step of the proposed approach.

Fig. 7 shows the areas corresponding to the clusters shown in Fig. 6. It can be seen from this figure that the test system has been partitioned into two distinct areas in Fig. 7(b) meaning that the right side (NETS) oscillates against the left side (NYPS) following this disturbance. However, as we look to the system from the view of NETS (Fig. 7(a)), virtual

Table 3
Load shedding results (case 2).

	Scheme 1			Scheme 2		Scheme 3		Scheme 4		
	Area 1	Area 2	Area 3	Area 1	Area 2	Area 1	Area 2	Area 1	Area 2	Area 3
Load shedding in each area (MW)	0	15	0	0	5.6	0	5.6	0	0	0
Total (MW)	15			5.6		5.6		0		

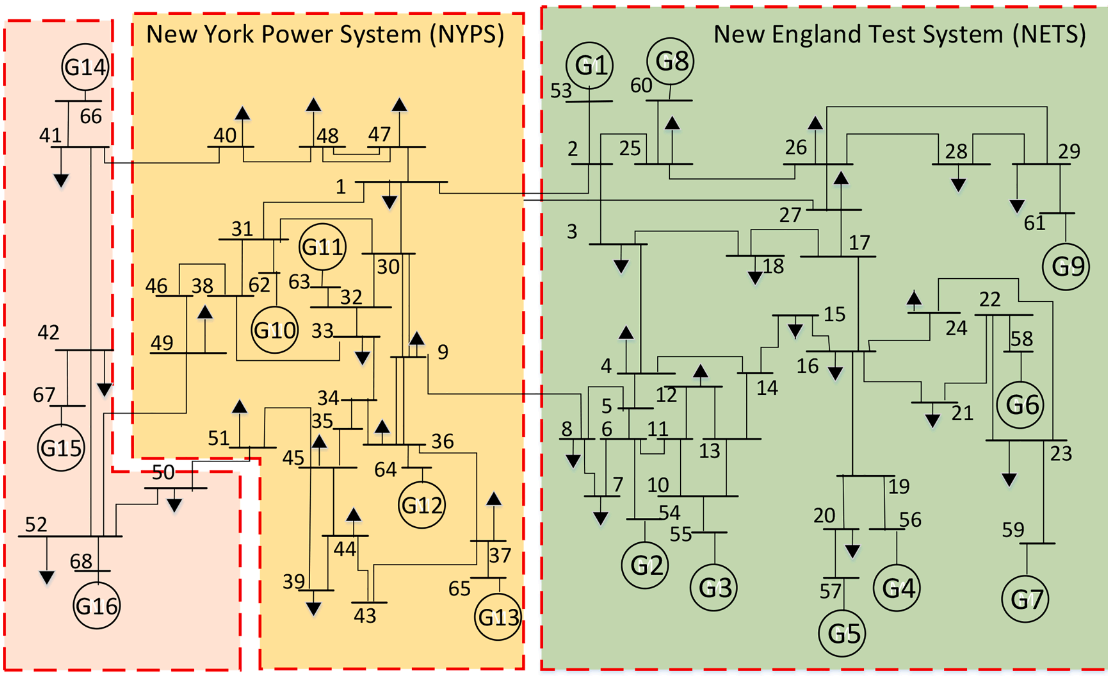

Fig. 11. Areas identified by coherency evaluation method in [8].

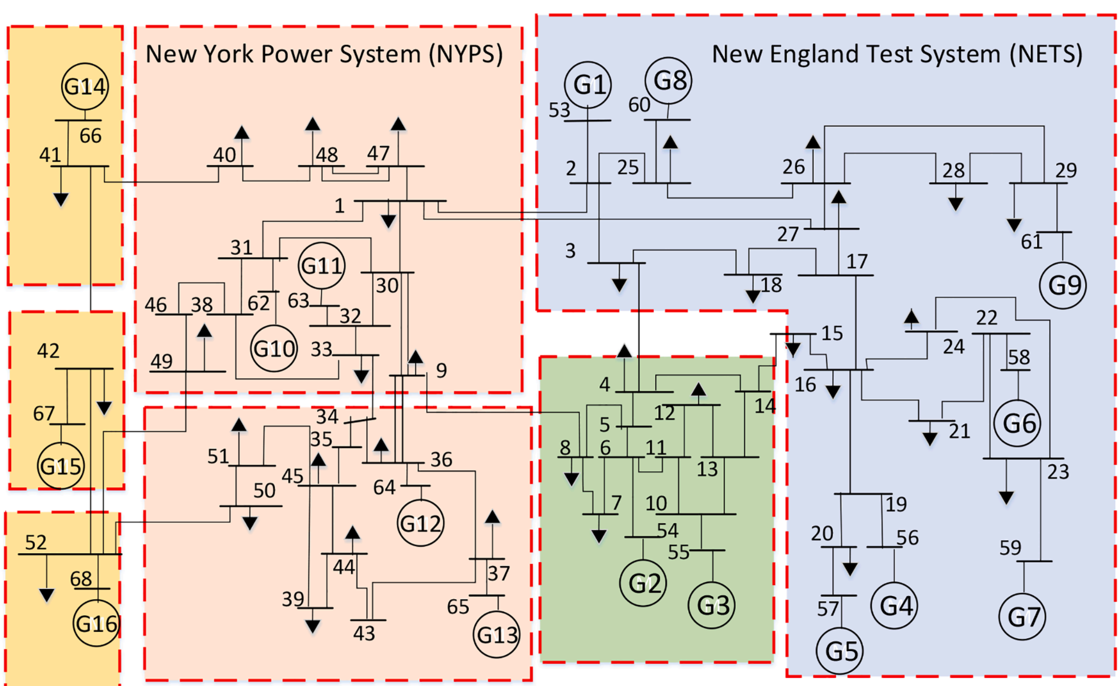

Fig. 12. Splitting strategy identified by the method presented in [28].

generators, i.e. Gens 14, 15 and 16, which are connected to NYPS, can form a distinct area as well.

The load shedding solution applied to each of the separation schemes are tabulated in Table 2. It can be seen that the second separation scheme, which associates with Fig. 6(b), is the best in this case since very low load shedding is required in this scheme. In fact, in response to this fault, large virtual generators, i.e. generators 14, 15 and 16, have revealed responses relatively similar to real generators in NYPS. Therefore, retaining their connection to NYPS can help in achieving a better solution in terms of lower load shedding, while the dynamics of elements within the area are relatively similar.

Fig. 8 shows the speed variations of generators G1 – G9 which are in the right side of the test system. As it can be seen, these generators reveal approximately the same variations in response to the disturbance. There are also several local oscillations that are damped in the first two seconds following disturbance occurrence. These modes are not seen as we have set α on 0.15. In order to include these modes and consider local oscillation frequencies one could consider a smaller value for α.

3.2. Case 2

The aim of this case is to show that the proposed method can work well for different cases. In this case, a 3-phase fault is applied to the line between buses 12 and 11 and near to bus 12 and it is cleared after 0.3 s. Fig. 9 depicts the data points in complex planes and the clusters obtained by applying DBSCAN to the data points in each complex plane. It is found that buses 33, 26, 11, 42 and 23 have been identified as the cluster centers in this case. As Fig. 9 shows, four splitting schemes have been found as the candidate schemes, which should be further analyzed. Fig. 10 shows the areas of the system corresponding to the clusters obtained in Fig. 9.

Table 3 tabulates the details of the minimum load shedding required in each scheme. Note that the order of splitting schemes in Table 2 corresponds to the order of sub-figures (a) to (d) shown in Fig. 10. As observed, Scheme 4, which corresponds to the system splitting scheme shown in Figure 10(d), has the best solution, since the lowest amount of load shedding is required in this scheme. Note that, another conclusion drawn from comparing this case and Case 1 is that an online coherency evaluation is indispensable for controlled islanding, and dependence on fixed coherent groups obtained through slow-coherency concept cannot be reliable.

3.3. Discussion and additional notes

In this Section, comparisons made between the proposed method and several methods presented in the literature is provided. In the first part, the features of the proposed coherency evaluation approach over other methods are highlighted. To do that, results obtained in Case 1 are compared with the results obtained from using the method presented in [8]. It should be noted that the reason for selecting these methods is that, like our proposed method, the method in [8] tries to evaluate the coherency on the buses of the system rather than on generators' rotor angle variations. By applying the coherency evaluation method presented in [8], areas will be identified as shown in Fig. 11. As it can be seen from this figure, although there is a slight difference between Fig. 11 and Fig. 7(a), it is different from the final solution in Case 1. Moreover, it should be noted that the areas identified by [8] are the outcome of a coherency evaluation process and no load shedding strategy is involved. In contrast, the areas shown in Fig. 7(b), which are the outcome of the proposed method, is the splitting strategy through which the final load shedding scheme is determined as well.

In the second part, another comparison is made between the final splitting results in Case 2 and the results obtained through applying the method presented in [28] (with the exception that the effects of renewable generation in [28] have been excluded). Fig. 12 shows the islanding strategy that is identified in the solution obtained by the method in [28]. The total load shedding that this islanding strategy proposes is 9.8 MW, which is greater than the 5.6 MW obtained by using our proposed method. This is a strong verification of what we discussed in Section I. As discussed, the final load shedding solution of the methods in [28] or [35] is highly dependent to the coherent groups of generators that has been identified in the first step. In this regard, since only a specific generators grouping scheme is proposed as the input for the second step, there would be a smaller search space for optimization problem in the second step. However, in the proposed approach a set of candidate splitting strategies is proposed in the first step, and therefore the optimization problem faces more flexibility in terms of load shedding, which is a great advantage of the proposed approach.

In fact, there is a big difference between the proposed approach and the rest of similar approaches in the literature and that is in our proposed approach the coherency evaluation process and system load shedding determination are not separated from each other. In other words, using the method proposed in this paper an area identification solution solely on the basis of coherency will not be obtained. As shown through the simulations of Cases 1 and 2, by using the proposed approach a set of candidate splitting strategies on the basis of coherency evaluation is obtained and then the final strategy is selected after the load shedding strategy is specified. This means that, unlike methods presented in [28] and [35] in which a specific generators grouping is determined in the first step, in our proposed approach the specific areas are identified after the step 2 (optimal load shedding strategy determination) is carried out as well.

It should also be noted that, since the identified islanding solution assures the coherency of generators in each area as well as the balance between generation and load, each island expected to be stable after islanding is applied. However, in order to show that each area remains stable after system separation it is needed to apply the system separation after disturbance occurrence. But, the question is when to apply? The answer to this question is out of scope of this paper and is considered as a suggestion for future works. In fact, the aim of the proposed methodology is to find the solution for the controlled islanding if a controlled islanding becomes essential.

There are additional notes that should be taken into account. First, The cases simulated above were chosen to demonstrate how the proposed approach reaches the final solution in response to different types of disturbance. It should be noted that in the above cases, it was not simulated how controlled islanding could prevent the probable system collapse. Indeed, it was not the aim of this paper to apply the controlled islanding solution to the system. Certainly, a controlled islanding strategy could be appropriate and successful if it is triggered on time and is performed in a way that retains both the dynamic and static stability of each island.

Secondly, the proposed islanding approach splits the system into islands, so that lower amount of load shedding in each island is needed to maintain the static and dynamic stability of each island. Therefore, the time at which the controlled islanding strategy should be detected to create islands; this has been investigated in research studies such as [48] and [49], and is out of the scope of this paper. Accordingly, although a 10-second time frame is assumed in this paper for data measurement required for coherency evaluation after disturbance occurrence, in reality, the end of this time frame is the time at which creating islands is essential to prevent the propagation of disturbance effects into the system.

4. Conclusion

In this paper, a novel approach was presented to obtain a solution for online controlled islanding. In the proposed approach, an innovative online coherency evaluation in the complex domain was incorporated into a much simpler load shedding optimization problem. Unlike previous works in which the emphasis was on the static characteristics of the system when finding the controlled islanding solution, the proposed approach emphasized the dynamics of the system. The reason is that for tuning controllers during the islanded power system and for the system restoration, it is more important to determine the borders of islands based on the propagation of responses of generators in the system following a disturbance. The results of applying the proposed approach on different cases of a standard test system indicate that it can effectively find the best solution with very low amount of load shedding. Moreover, the method is fast as it is much simpler than other optimization approaches in the literature and is suitable for online applications.

The method presented in this paper solely determines the islanding strategy if islanding becomes required for given a disturbance occurrence, which means that the necessity for islanding was not included. Future works on this topic are therefore recommended in order to establish a more general framework by which, along with the islanding strategy determination, the necessity to perform islanding is also detected on the basis of putting the priority on the dynamics of the system.

Authorship statement

All persons who meet authorship criteria are listed as authors, and all authors certify that they have participated sufficiently in the work to take public responsibility for the content, including participation in the concept, design, analysis, writing, or revision of the manuscript. Furthermore, each author certifies that this material or similar material has not been and will not be submitted to or published in any otherpublication before its appearance in the journal of Electric Power Systems Research.

Authorship contributions

Please indicate the specific contributions made by each author. The name of each author must appear at least once in each of the three categories below.

Category 1

Conception and design of study: Akbari Hamidreza; Sadeghi Mohamadsadegh acquisition of data: Sadeghi Mohamadsadegh analysis and/or interpretation of data: Akbari Hamidreza, Sadeghi Mohamadsadegh, Daemi Tahereh, Mousavi Somayeh.

Category 2

Drafting the manuscript: Akbari Hamidreza; Sadeghi Mohamadsadegh revising the manuscript critically for important intellectual content:

Akbari Hamidreza

Category 3

Approval of the version of the manuscript to be published (the names of all authors must be listed):

Sadeghi Mohamadsadegh, Akbari Hamidreza, Daemi Tahereh, Mousavi Somayeh.

Declaration of Competing Interest

The authors declare that they have no known competing financial interests or personal relationships that could have appeared to influence the work reported in this paper.

Acknowledgements

All persons who have made substantial contributions to the work reported in the manuscript (e.g., technical help, writing and editing assistance, general support), but who do not meet the criteria for authorship, are named in the Acknowledgements and have given us their written permission to be named. If we have not included an Acknowledgements, then that indicates that we have not received substantial contributions from non-authors.

References

[1] A. Ghasempour, "Advanced metering infrastructure in smart grid: requirements, challenges, architectures, technologies, and optimizations," in Smart Grids: Emerging Technologies, Challenges and Future Directions, Nova Science Publishers, pp. 77–127, 2017.

[2] N. Senroy, G.T. Heydt, A conceptual framework for the controlled islanding of interconnected power systems, IEEE Trans. Power Syst. 21 (2) (2006) 1005–1006.

[3] B. Yang, V. Vittal, G.T. Heydt, Slow-coherency-based controlled islanding—a demonstration of the approach on the August 14, 2003 blackout scenario, IEEE Trans. Power Syst. 21 (4) (2006) 1840–1847.

[4] M. Mishra, M. Sahani, P.K. Rout, An islanding detection algorithm for distributed generation based on Hilbert–Huang transform and extreme learning machine, Sustainable Energy, Grids and Networks, 9 (2017) 13–26.

[5] M. Rezaee, M.S. Moghadam, M. Shokouhinia, S. Ranjbar, Online estimation of power system separation as controlled islanding scheme in the presence of inter-area oscillations, Sustainable Energy, Grids and Networks 21 (2020), 100306.

[6] B. Mehdi, S.M. Muyeen, I. Syed, Transiently stable intentional controlled islanding considering post-islanding voltage and frequency stability constraints, Int. J. Electrical Power and Energy Syst. 127 (2021), 106650.

[7] M.H.R. Koochi, S. Esmaeili, P. Dehghanian, Coherency detection and network partitioning supported by wide area measurement system, IEEE Texas Power and Energy Conference (TPEC), USA (2018).

[8] M.H. Rezaeian, S. Esmaeili, R. Fadaeinedjad, 'Generator coherency and network partitioning for dynamic equivalencing using subtractive clustering algorithm, IEEE Syst J 12 (2018) 3085–3095.

[9] Ourari, M., Dessaint, L., Do, V.: 'Coherency approach for dynamic equivalents of large power systems'. Int. Conf. Power Systems Transients – IPST, New Orleans, LA, USA, pp. 1–6, 2003.

[10] Z. Lin, F. Wen, Y. Ding, Data-driven coherency identification for generators based on spectral clustering, IEEE Trans. Ind. Inf. 14 (2018) 1275–1285.

[11] S. Jafarzadeh, I. Genc, Nehorai, A. Real-time transient stability prediction and coherency identification in power systems using Koopman mode analysis, Electr. Power Syst. Res. 201 (2021), 107565.

[12] K. Mandadi, B.K. Kumar, Generator coherency using Zolotarev polynomial based filter bank and principal component analysis, Int. J. Emerg. Electr. Power Syst. 19 (2018) 1–13.

[13] A.M. Khalil, R. Iravani, 'A dynamic coherency identification method based on frequency deviation signals, IEEE Trans. Power Appar. Syst. 31 (2016) 1779–1787.

[14] T. Jiang, H. Jia, H. Yuan, 'Projection pursuit: a general methodology of wide-area coherency detection in bulk power grid, IEEE Trans. Power Appar. Syst. 31 (2016) 2776–2786.

[15] M.H.R. Koochi, S. Esmaeili, G. Ledwich, Taxonomy of coherency detection and coherency-based methods for generators grouping and power system partitioning, ET Gener. Transm. Distrib. 13 (12) (2019) 2597–2610.

[16] J. Li, C. Liu, K.P. Schneider, Controlled partitioning of a power network considering real and reactive power balance, IEEE Trans Smart Grid 1 (3) (Dec. 2010) 261–269.

[17] C.G. Wang, B.H. Zhang, Z.G. Hao, J. Shu, P. Li, Z.Q. Bo, A novel real-time searching method for power system splitting boundary, IEEE Trans. Power Syst. 25 (4) (2010) 1902–1909.

[18] T. Ding, H. Sun, K. Sun, F. Li, X. Zhang, Graph theory based splitting strategies for power system islanding operation, 2015 IEEE Power & Energy Society General Meeting (2015) 1–5.

[19] G. Isazadeh, A. Khodabakhshian, E. Gholipour, New intelligent controlled islanding scheme in large interconnected power systems, ET Gener. Transm. Distrib. 9 (16) (2015) 2686–2696.

[20] L. Ding, Z. Ma, P. Wall, V. Terzija, Graph Spectra Based Controlled Islanding for Low Inertia Power Systems, IEEE Trans. Power Delivery 32 (1) (2017) 302–309.

[21] S. Daniar, F. Aminifar, M.R. Hesamzadeh, H Lesani, Optimal controlled islanding considering frequency-arresting and frequency-stabilising constraints: a graph theory-assisted approach, IET Gener. Transm. Distrib. 15 (2021) 2044–2060.

[22] T. Amraee, H. Saberi, Controlled islanding using transmission switching and load shedding for enhancing power grid resilience, Int. J. Electr. Power Energy Syst. 91 (2017) 135–143.

[23] P.A. Trodden, W.A. Bukhsh, A. Grothey, K.I. McKinnon, Optimization-based islanding of power networks using piecewise linear AC power flow, IEEE Trans. Power Syst. 29 (3) (2014) 1212–1220.

[24] T. Ding, K. Sun, C. Huang, Z. Bie, F. Li, Mixed-integer linear programming-based splitting strategies for power system islanding operation considering network connectivity, IEEE Syst. J. 12 (1) (Mar. 2018) 350–359.

[25] E. Saadipour-Hanzaie, T. Amraee and S. Kamali, "Minimal controlled islanding with similarity-based coherency identification using phasor measurement data," in *IEEE Transactions on Industrial Informatics*, vol. 18, no. 5, pp. 3256–3266, May 2022, doi: 10.1109/TII.2021.3105180.

[26] S. Liu, T. Zhang, Z. Lin, Y. Liu, Y. Ding, L. Yang, Controlled islanding strategy considering uncertainty of renewable energy sources based on chance-constrained model, J. Modern Power Syst. Clean Energy 10 (2) (March 2022) 471–481.

[27] T. Ding, K. Sun, Q. Yang, A.W. Khan, Z. Bie, Mixed integer second order cone relaxation with dynamic simulation for proper power system islanding operations, IEEE J. Emerg. Sel. Top Circuits Syst. 7 (2) (Jun. 2017) 295–306.

[28] S.Y. Liu, Z.Z. Lin, Y.X. Zhao, Y.L. Liu, Y. Ding, B. Zhang, L. Yang, Q. Wang, S. E. White, Robust system separation strategy considering online wide-area coherency identification and uncertainties of renewable energy sources, IEEE Trans. Power Syst. 35 (5) (Sep. 2020) 3574–3587.

[29] A. Golshani, W. Sun, K. Sun, An advanced power system partitioning method for fast and reliable restoration: towards a self-healing power grid, ET Gener. Transm. Distrib. (2017).
[30] L. Ding, Y. Guo, P. Wall, Performance and suitability assessment of controlled islanding methods for online WAMPAC application, Int. J. Electr. Power Energy Syst. 84 (2017) 252–260.
[31] S. Basumallik, S. Eftekharnejad, M. Fardad, Controlled islanding under complete and partial false data injection attack uncertainties against phasor measurement units, Energies 15 (2022) 5723.
[32] Z. Sun, Y. Spyridis, T. Lagkas, A. Sesis, G. Efstathopoulos, P. Sarigiannidis, End-to-end deep graph convolutional neural network approach for intentional islanding in power systems considering load-generation balance, Sensors 21 (2021) 1650.
[33] G. Xu, V. Vittal, Slow coherency based cutset determination algorithm for large power systems, IEEE Trans. Power Syst. 25 (2) (May 2010) 877–884.
[34] F. Raak, Y. Susuki, T. Hikihara, Data-driven partitioning of power networks via Koopman mode analysis, IEEE Trans. Power Syst. 31 (4) (Jul. 2016) 2799–2808.
[35] F. Teymouri, T. Amraee, H. Saberi, F. Capitanescu, Towards controlled islanding for enhancing power grid resilience considering frequency stability constraints, IEEE Trans Smart Grid 10 (2) (Mar. 2019) 1735–1746.
[36] F. Teymouri, Amraee, T. An MILP formulation for controlled islanding coordinated with under frequeny load shedding plan, Electr. Power Syst. Res. 171 (2019) 116–126.
[37] M. Golari, N. Fan, J. Wang, Two-stage stochastic optimal islanding operations under severe multiple contingencies in power grids, Electr. Power Syst. Res. 114 (2014) 68–77.
[38] H.A. Alsafih and R. Dunn, “Determination of coherent clusters in a multi machine power system based on wide-area signal measurements,” in *Proc. IEEE Power Energy Soc. Gen. Meeting*, 2010, pp. 1–8.
[39] I. Kamwa, A.K. Pradhan, G. Joos, S. Samantaray, Fuzzy partitioning of a real power system for dynamic vulnerability assessment, IEEE Trans. Power Appar. Syst. 24 (3) (Aug. 2009) 1356–1365.
[40] M. Ester, H.-.P. Kriegel, J. Sander, X. Xu, A density-based algorithm for discovering clusters in large spatial databases with noise, in: Proceedings of 2nd International Conference on KDD, 1996, pp. 226–231, pages.
[41] J.G. Proakis and D.G. Manolakis, Digital signal processing principles algorithms and applications, 1996.
[42] N.S. Neidell, M.T. Taner, Semblance and other coherency measures for multichannel data, Geophysics 36 (1971) 482–497.
[43] M. Taner, "Semblance and Other Similarity Measurements", Rock Solid Images, pp. 1–4, 1996.
[44] K. Hammouda and F. Karray, “A comparative study of data clustering techniques,” Waterloo, ON, Canada: Fakhreddine Karray Univ, 2000.
[45] G. Rogers, *Power System Oscillations*. Springer Science & Business Media, 2012.
[46] Power System Toolbox (PST), available online at http://www.eps.ee.kth.se/personal/vanfretti/pst/Power_System_Toolbox_Webpage/PST.html.
[47] S.L. Chiu, Fuzzy model identification based on cluster estimation, J. Intell. Fuzzy Syst. 2 (1994) 267–278.
[48] L. Ding, Y. Guo, P. Wall, K. Sun, V. Terzija, Identifying the timing of controlled islanding using a controlling UEP based method, IEEE Trans. Power Syst. 33 (6) (Nov. 2018) 5913–5922.
[49] S. Kamali, T. Amraee, S.M. Bathaee, Prediction of unplanned islanding using an energy based strategy, ET Gener. Transm. Distrib. 10 (1) (Jan. 2016) 183–191, vol.